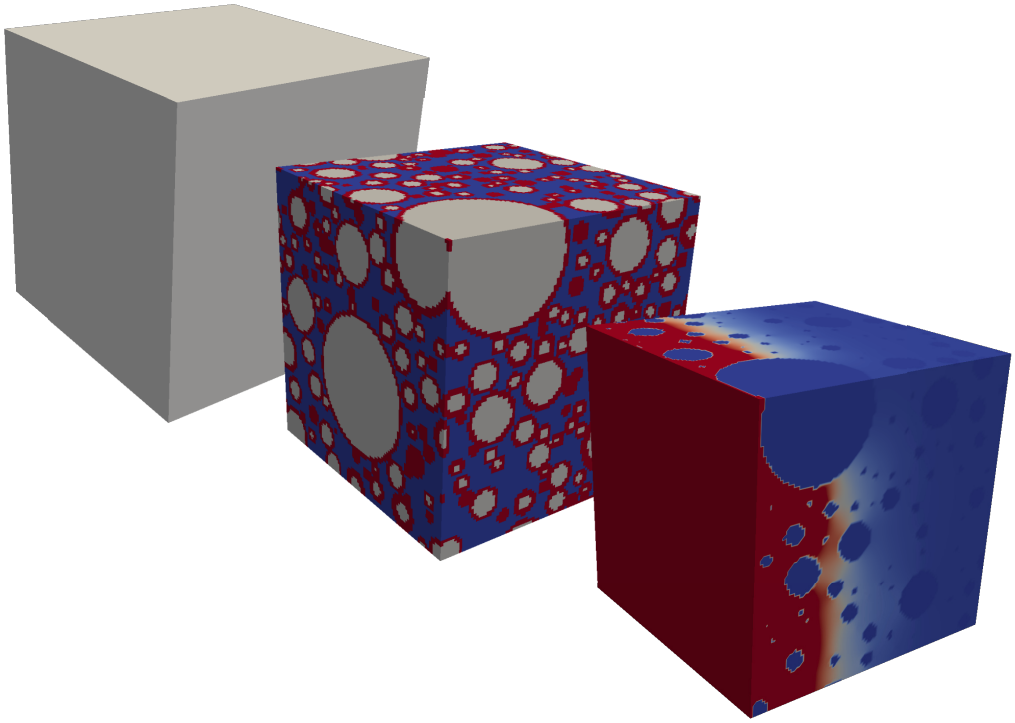

Finite Element Model Evaluation using Factorial Design

Simulation of Chloride diffusion in 3D heterogeneous concrete

Master's thesis in Structural Engineering and Building Technology

HOSSEIN TAHERSHAMSI

Department of Civil and Environmental Engineering
Division of Structural Engineering
Concrete Structures
CHALMERS UNIVERSITY OF TECHNOLOGY
Gothenburg, Sweden 2017

Master's thesis BOMX02-17-48

MASTER'S THESIS BOMX02-17-48

Finite Element Model Evaluation using Factorial Design

Simulation of Chloride diffusion in 3D heterogeneous concrete

Master's thesis in Structural Engineering and Building Technology

HOSSEIN TAHERSHAMSI

Department of Civil and Environmental Engineering
Division of Structural Engineering
Concrete Structures
CHALMERS UNIVERSITY OF TECHNOLOGY

Gothenburg, Sweden 2017

Finite Element Model Evaluation using Factorial Design
Simulation of Chloride diffusion in 3D heterogeneous concrete
HOSSEIN TAHERSHAMSI

Master's thesis BOMX02-17-48
ISSN 1652-8557
Department of Civil and Environmental Engineering
Division of Structural Engineering
Concrete Structures
Chalmers University of Technology
SE-412 96 Gothenburg
Sweden
Telephone: +46 (0)31-772 1000

Colophon:
The thesis was created using LaTeX 2_ε and `biblatex` and edited in `Texmaker`. The typesetting software was the TeX Live distribution. The text is set in Times New Roman. Graphs were created using PGFPLOTS. Figures were created using INKSCAPE.

Cover:
Three dimensional heterogeneous and solid model of concrete including transient diffusion in a 4 cm SVE, visualized by ParaView.

Chalmers Reproservice
Gothenburg, Sweden 2017

Finite Element Model Evaluation using Factorial Design
Simulation of Chloride diffusion in 3D heterogeneous concrete
Master's thesis in Structural Engineering and Building Technology
HOSSEIN TAHERSHAMSI
Department of Civil and Environmental Engineering
Division of Structural Engineering
Concrete Structures
Chalmers University of Technology

ABSTRACT

Concrete structures should be capable of withstanding the conditions throughout the serviceability of the structure. Due to the exposure of the external agents arising from the environment e.g. chloride ions, concrete structures will gradually deteriorate. Transport of chloride ions in concrete is a complex phenomenon which is hard to predict and model. However, modelling is highly preferable as a means for assessing and predicting the behaviour of existing concrete structures, such as bridges.

The behaviour of such models, nevertheless, need to be evaluated as a prediction tool in order to optimise cost and time of experimental studies. The general aim is to perform a statistical method called "factorial design" on sets of outputs taken from a 3D heterogeneous concrete model. The obtained results are used to observe the main effects and interactions of different factors.

Two different cases of chloride transport are investigated: stationary and transient diffusion. The analysis of stationary case shows a proper relation between aggregate content and Interfacial Transition Zone(ITZ) diffusivity. A resolution IV fractional factorial was designed for six factors of the transient model. The data shows that more gravel content increases the time for chloride ions to reach the chloride threshold. Three dominant parameters- gravel content, cement storage capacity and cement diffusivity- were screened to perform a full factorial design. No specific interactions were observed among the three studied parameters. However, the influence of higher order interactions were noticed between the fractional and full factorial design.

Keywords: Diffusion, FE simulation, Factorial design, Computational homogenization, Concrete

CONTENTS

PREFACE

This MSc thesis was carried out at the Division of Structural Engineering, Department of Civil and Environmental Engineering, Chalmers University of Technology from January until June 2017.

I would like to express my sincere gratitude to my supervisor and examiner, Assistant Professor Filip Nilenius. I really enjoyed and benefited enormously from our discussions to develop this project. I also want to thank him for taking the time to update part of his codes to facilitate and reduce total run time of the model.

I would like to express my appreciation to all my teachers at the Division of Structural Engineering and Applied Mechanics. Martin Fagerström, Ragnar Larsson and Björn Engström, I really enjoyed your lectures and learned a lot. My friends at Chalmers, you know who you are, I had a really nice time at here thanks to you.

Mikael Öhman at C3SE is acknowledged for his assistance concerning technical comments in enhancing my batch file to run the code in parallel on the C3SE resources.

Lastly, I would like to thank particularly two people and they are my parents. My mother, a powerful strong woman, who I aspire to be each and every single day. My father, a great mentor, who taught me the value of hardwork. Without them, I would never have gotten to where I am today. I would also like to thank my siblings, for their encouragement and support during my studies.

Gothenburg, 2017
Hossein Tahershamsi

Acronyms

3D three-dimensional. 1

CSH calcium silicate hydrate. 3

FE Finite Element. 1

HCP hardened cement paste. 3

ITZ Interfacial Transition Zone. 3

NEL Number of Elements. 16

OOP Object-Oriented programming. 4

SVE Statistical Volume Element. 1

Nomenclature

Subscripts

b	aggregate
cp	cement paste
int.	factorial design interaction effect
ITZ	Interfacial Transition Zone
main.	factorial design main effect

Greek letters

$\boldsymbol{C_M}$	factorial design contrast matrix
ρ_H	stored chloride content (kg/m^3)
α	convective coefficient (m s^{-1})
ΔC_{dev}	concrete cover deviation (mm)
$\Delta C_{\text{dur,add}}$	reduction of minimum cover for use of additional protection (mm)
$\Delta C_{\text{dur},\gamma}$	additive safety element (mm)
$\Delta C_{\text{dur,st}}$	reduction of minimum cover for use of stainless steel (mm)
Φ	storage capacity (-)

Roman lower case letters

$\boldsymbol{n}$	normal vector
c	Chloride ion concentration (kg/m^3)
$\boldsymbol{q}$	Ion flux vector (kg/m^{2}s)
C_{min}	minimum concrete cover (mm)
$C_{\text{min,b}}$	bond requirement minimum cover (mm)
$C_{\text{min,dur}}$	minimum cover due to environmental conditions (mm)
$\boldsymbol{a}$	nodal values
C_{nom}	nominal concrete cover (mm)
n_b	Gravel content (-)
nx	number of elements along each side of SVE

Roman capital letters

$\boldsymbol{E}$	factorial design vector of main and interaction effects
$\boldsymbol{R}$	factorial design response vector
$\boldsymbol{D}$	Constitutive matrix for diffusion coefficient
Q	Chloride ion supply (kg/m^{3}s)

D_{cp} Diffusivity of cement paste ($cm^2\ year^{-1}$)
D_{ITZ} Diffusivity of ITZ ($cm^2\ year^{-1}$)
$L_{\square}$ side length of SVE (cm)

1 Introduction

1.1 Background

Many recent studies have concentrated on corrosion of embedded reinforcement in concrete considering structural assessment and durability of existing concrete structures (Blomfors et al., 2017; Tahershamsi et al., 2014; Lundgren, 2007). Concrete should be capable of withstanding the conditions throughout the serviceability of the structure. Due to the exposure of the external agents arising from the environment e.g. chloride ions, concrete structures will gradually deteriorate. This leads to reduction of load carrying capacity of the structure and therefore increase the repair and maintenance costs. The source of the chloride ions are from the de-icing salts or marine environments. For instance, bridge decks, parking garage floors and marine structures are in risk of chloride attack.

Nilenius (2014) carried out an extensive simulation of heterogeneous concrete and utilise the model for computational mass transport phenomena in concrete. In particular, a Statistical Volume Element (SVE) of concrete representing the heterogeneous mesoscale structure and non-linearity of the material was developed. The SVE has represented the mass transport in concrete on the macroscale. However, the correlation of mass transport model in conjunction with experimental studies related to transport properties of concrete remains unclear.

1.2 Problem description

Mass transport process in concrete is a highly complex phenomenon which is hard to predict and model. However, modelling the phenomenon is considered as a means for assessing the performance of concrete in existing structures.

In order to make good predictions using models, the simulations need to be accurately calibrated with experimental data. Such calibrations are complicated since there are different numbers of parameters which are implemented into the model. Several sources of uncertainty exist within the input and output of the model. Therefore, evaluation of the model in terms of sensitivity of different parameters before calibration is crucial.

1.3 General aim

The aim of the thesis is to perform a statistical method on sets of outputs taken from a three-dimensional (3D) Finite Element (FE) model of heterogeneous concrete (Nilenius, Larsson, et al., 2014a; Nilenius, Larsson, et al., 2014b). The results obtained from the simulations are used to observe main effects and interactions of different factors. Stationary and transient cases of diffusion are investigated. Exploration of the dominant parameters within the two models is another intention of this study.

1.4 Methodology and scientific approach

Figure 1.1 shows the methodology used in this thesis. The different steps of the study are listed as follows:

(i) Conduct literature review about the physics of mass transport phenomenon in concrete and the statistical method called "factorial design".

(ii) Review the 3D Finite Element model of heterogeneous concrete which was constructed to model the transport phenomenon.

(iii) Conduct the mathematical and Finite Element formulation of chloride ingress.

(iv) Design the experiments using factorial sampling by implementing into the 3D Finite Element model.

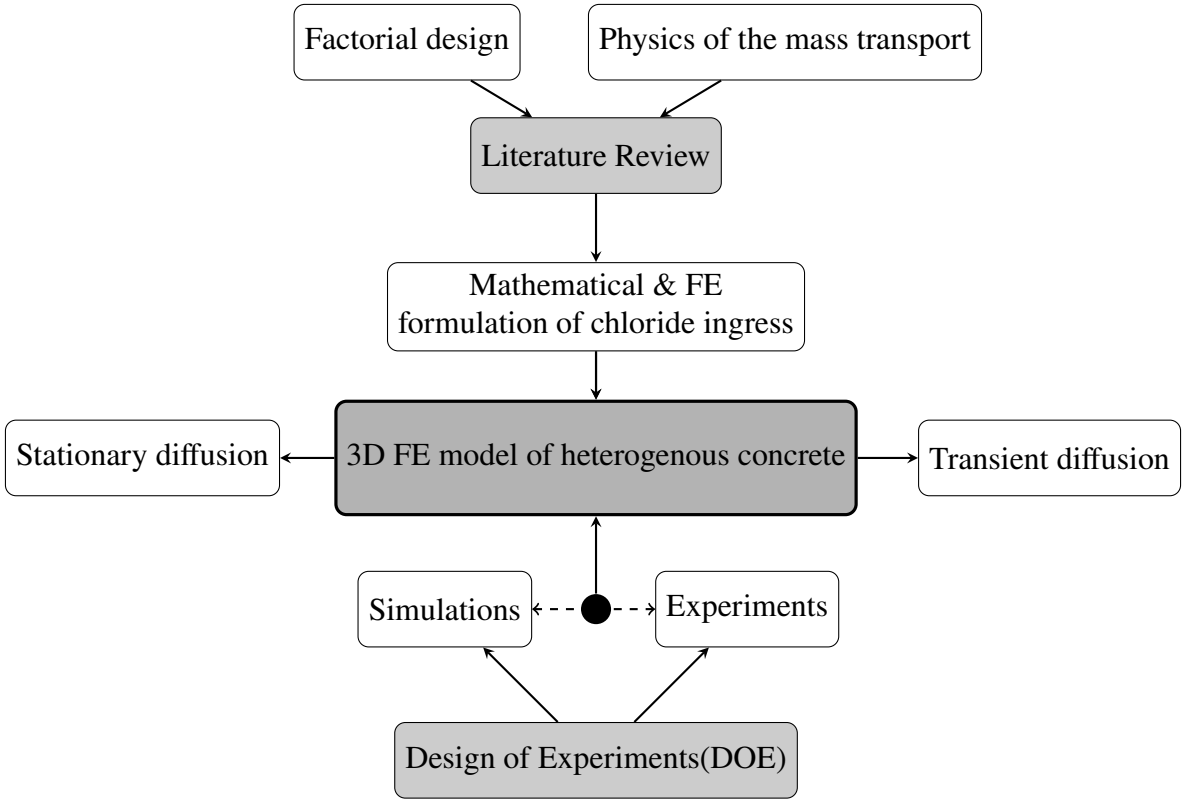

Figure 1.1: *Methodology of the study.*

1.5 Scope and limitations

Throughout this study, only Dirichlet boundary condition is used for the FE formulation of the stationary diffusion. Moreover, only limited chloride ingress experimental studies has been conducted. Most of

them have different experimental approach and results in diverse dimensions of the parameters. Therefore, choosing the same parametric values with respect to previous studies is challenging.

2 Mass transport in concrete

2.1 Concrete as a material

Concrete is a composite material produced by the reaction between hydraulic cement and water. However, it can be followed by additional admixtures and a wide range of products. Hydrated cement paste, aggregate, and interfaces between them are mainly phases of the concrete.

According to Neville and Brooks (2010) Portland cement, as the most common type, consists of four primary components: C_3S, C_2S, C_3A and C_4AF. These components play an important role in the hydration process of the cement. In presence of water, cement grains are dispersed in water. The hydration products, ettringite and calcium silicate hydrate (CSH), are formed on the surface of the grains. This process leads to the formation of hardened cement paste (HCP) which binds the aggregate together. Hydrated cement consists of capillary voids and therefore, it is a porous substance.

The aggregates mainly affect the durability and structural performance of concrete. In other words, they act as an inner filler in the concrete providing improved volume stability. There are wide ranges of classification regarding aggregates such as size, petrographic, shape, and texture which can be found in the work by Neville and Brooks (2010) and Černý and Rovnaníková (2002).

The interface between cement and ballast is referred to as the Interfacial Transition Zone (ITZ). The properties of the ITZ is different from the cement paste. ITZ is considered as a thin phase with high porosity. This high level of porosity results in higher diffusivity and lower stiffness compare to the cement paste (Nilenius, 2014).

2.2 Moisture transport

Moisture transport mechanism can be investigated under saturated and unsaturated conditions. Pressure gradients are the major driving forces in saturated conditions where all the cement pores are completely filled with water in the liquid phase. In terms of unsaturated conditions, moisture exists in two phases, i.e. liquid and vapour phase, at the same time. The main transport mechanism in the liquid phase is pressure gradients including capillary forces, whereas diffusion and convection are the driving forces in the vapour phase. These mechanisms are complex to distinguish between in practice and often act in combination with each other (Nilenius, 2014).

2.3 Chloride transport

Neville and Brooks (2010) have described the electro-chemical action set up by the absorption of chloride ions by concrete. This interaction results in corrosion of the embedded steel reinforcement and therefore reduces the cross sectional area of the reinforcement bar. Due to corrosion of the reinforcement bars, additional damage can be caused by rupture of concrete surrounding reinforcement.

Homan et al. (2016) explain reinforcement corrosion in concrete occurs when the chloride content in contact with the steel surface has come to a threshold value while the moisture content in the concrete is sufficiently high. Therefore, transport of chloride ions are naturally coupled to the transport of moisture. The dissolved chloride ions will ingress through different transport mechanisms from the surface of the concrete structure to the embedded reinforcement. Two different transport mechanisms are presented in the studies by Ababneh and Xi (2002) and Homan et al. (2016). Fully saturated and partially saturated conditions for moisture and chloride transport are suggested. All the voids in fully saturated concrete are completely filled with moisture. Therefore, the dominant mechanism for chloride-moisture transport is the chloride concentration gradient. In particular, the chloride concentration gradient initiate the chloride penetration and results in moisture movement in concrete. However, in partially saturated concrete, both the moisture and chloride concentration result in the moisture transport and chloride penetration. Herein the model developed by Nilenius (2014) assumes to capture the combination of mentioned transport types.

3 3D concrete model

Concrete has a heterogeneous nature on the mesoscale. The three-dimensional model of concrete is developed in combination with homogenization techniques and Finite Element method by Nilenius, Larsson, et al. (2014a). The code is developed within Object-Oriented programming (OOP) paradigm using MATLAB software. Any sort of output data from the code is visualized with ParaView (2017).

3.1 The object-oriented paradigm

Eckerdal (2006) describes the object-oriented paradigm as a fundamental abstract concept which includes *object* and *class*. Three main principals of skilful software programs are discussed, which are:

1. Reusability, which is the ability of a software product to be reused for new applications in whole or in part.

2. Extendibility is the adaptability of the software program to changes of specification. This is achieved by creating independent parts of code.

3. Cost-efficiency is the cost for developing or maintaining the programs. This includes correcting errors and changes in the code when the circumstances change.

These principals are featured in Object-oriented paradigm. Following the procedure in Eckerdal and Thuné (2005), an example from this study is given in order to clarify the concept of *object*. Consider the SVE of the homogeneous concrete as an object. It has one variable for aggregate fraction, one variable for the size of the mesh. However, *class* is a description of properties and behaviour of the object. Material properties of cement, aggregates and ITZ are denoted as examples of classes in this model.

3.2 Stationary model

The schematic diagram of the finite element model of the SVE is shown in Figure 3.1. The stationary model follows the procedure which is explained in Section 3.5. In short, the diffusion tensor from the Fick's law, Equation (3.30), is calculated while divergence of chloride ion concentration, ∇c, is considered as unity. The diffusion tensor is calculated as Equation (3.1). Figures 3.1b to 3.1d show the elements containing cement, aggregates and ITZ, respectively.

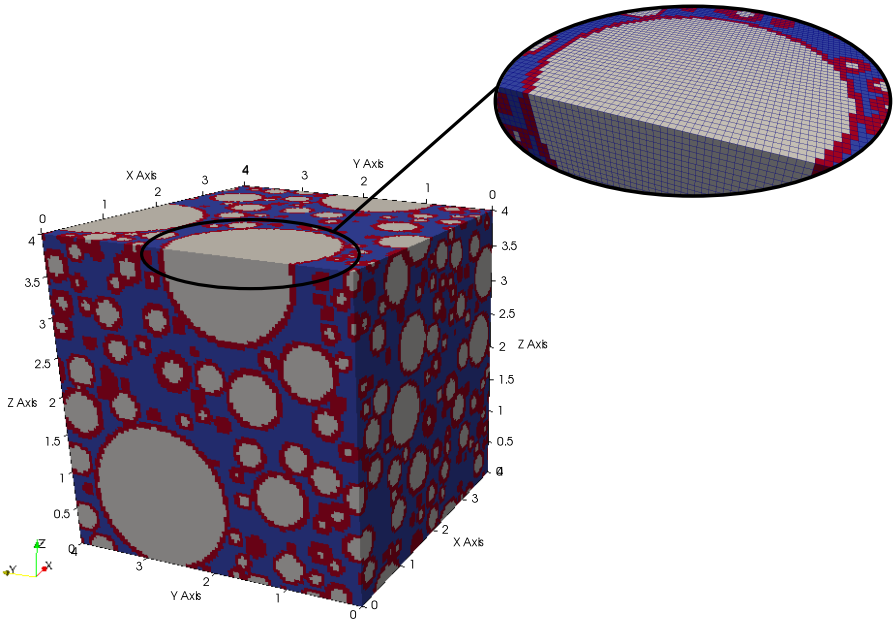

(a) *FE-discretized SVE.*

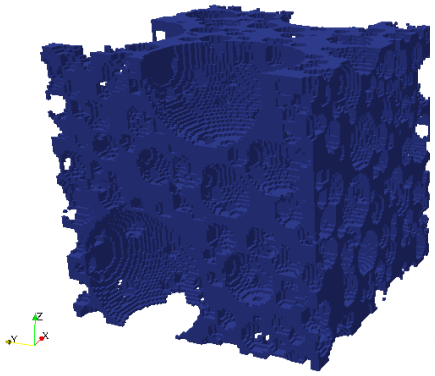

(b) *Cement elements.*

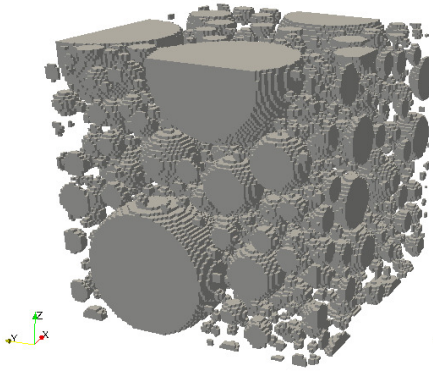

(c) *Aggregate elements.*

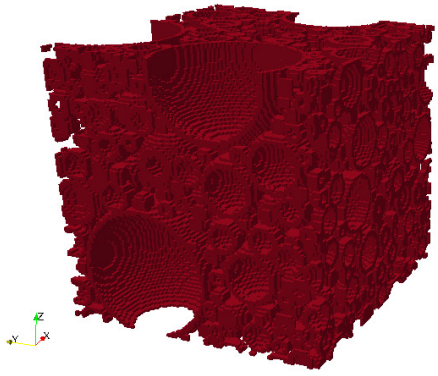

(d) *ITZ elements.*

Figure 3.1: *Example of a* $4(cm)$ *SVE with* $nx = 100$.

$$\boldsymbol{D} = \begin{bmatrix} D_{xx} & D_{xy} & D_{xz} \\ D_{yx} & D_{yy} & D_{yz} \\ D_{zx} & D_{zy} & D_{zz} \end{bmatrix} \tag{3.1}$$

3.3 Transient model

The transient model[†] follows FE-formulations which are derived in Section 3.4. Figure 3.2 present a case of chloride diffusion inside SVE. The SVE is isolated within the five sides of the cube and chloride can only diffuse through green arrow which represent the z-direction.

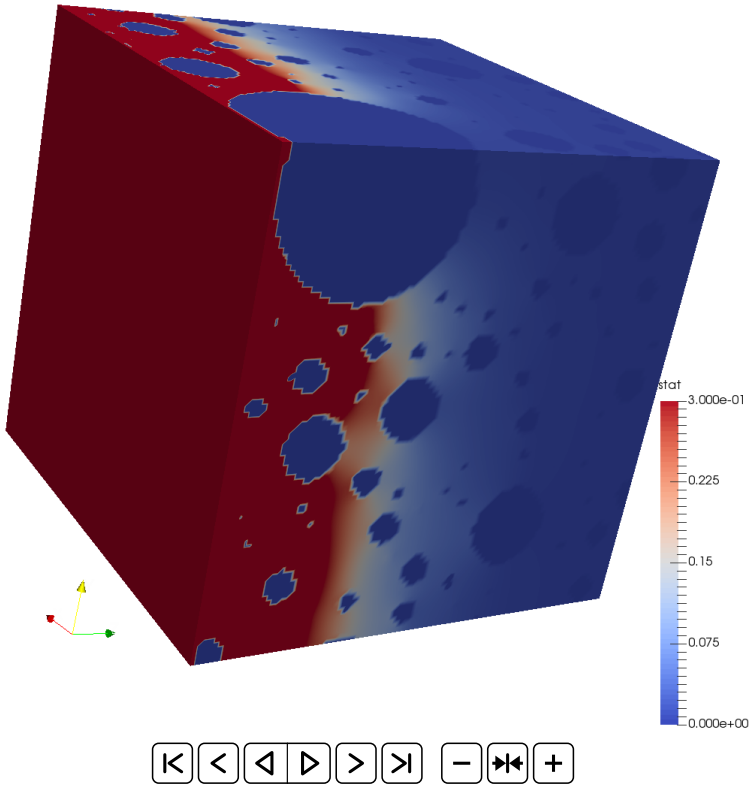

Figure 3.2: *Example of transient diffusion in a* 4(*cm*) *SVE. The color bar represent the chloride ion concentration.*

[†]Both the stationary and transient models are open source codes and are published in: `https://github.com/FilipNilenius/3D-concrete`

3.4 Transient diffusion FE-formulation

3.4.1 Strong and weak formulations

An arbitrary volume Ω with boundary Γ and outward normal $\boldsymbol{n}$ is considered. As it is presented in Figure 3.3, the outward flux on the boundary is a function of $\underline{\chi}$ and it can be written as Equation (3.2).

$$q_n = q_n(\underline{\chi}) = \boldsymbol{n}^T \boldsymbol{q}; \qquad \underline{\chi} = \begin{bmatrix} x \\ y \\ z \end{bmatrix} \tag{3.2}$$

As it was described in Chapter 2, the chloride ions are either moved because of the diffusion of ions inside the concrete or they are carried out through concrete voids coupled with moisture transport. For long-term exposure period, Ababneh and Xi (2002) states that moisture transport has no effect on chloride penetration and chloride concentration gradient is the most dominant mechanism. Thus, in this study, the concrete is assumed to be completely saturated and only the diffusion of chlorides are considered as a means of transport.

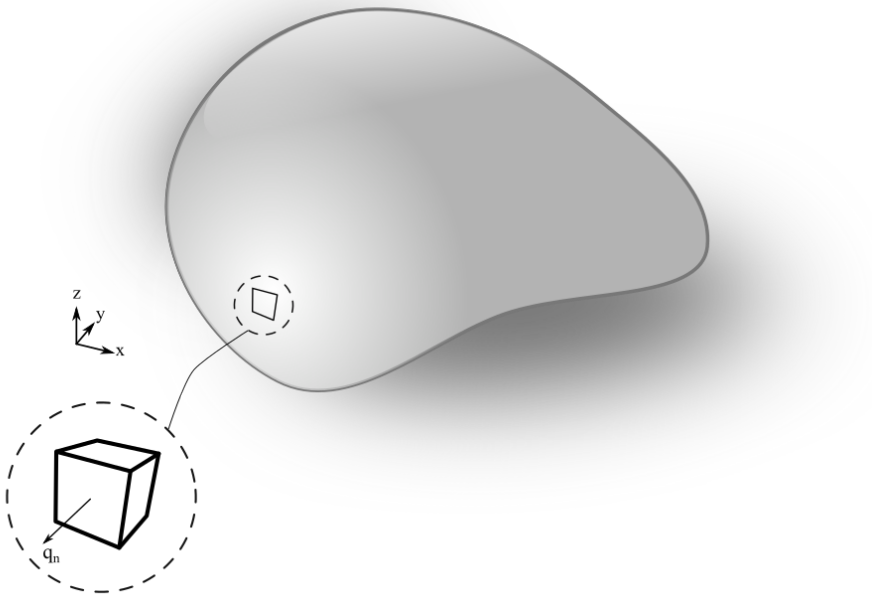

Figure 3.3: *Three-dimensional body located in xyz coordinate system presenting the flux q_n at the boundary.*

Consider mass of chloride ions per volume of the body represented in Figure 3.3. ρ_H is the stored chloride content within volume Ω and has dimensions of [kg m^{-3}]. Thus, it can be written as shown in Equation (3.3).

$$\rho_H = \rho_H(\underline{\chi}); \qquad \underline{\chi} = \begin{bmatrix} x \\ y \\ z \end{bmatrix} \tag{3.3}$$

The external chloride ion source Q [kg m^{-3} s^{-1}] is positive when the chloride is supplied to the body. However, there is no source of moisture or chloride supply inside the concrete in reality. Therefore, in Equation (3.4), Q is zero.

$$\frac{\partial}{\partial t}\int_\Omega \rho_H d\Omega = \int_\Omega Q d\Omega - \int_\Gamma q_n d\Gamma \tag{3.4}$$

The application of divergence theorem on the boundary integral in Equation (3.4) gives:

$$\frac{\partial}{\partial t}\int_\Omega \rho_H d\Omega = -\int_\Omega \mathrm{div}(\boldsymbol{q}) d\Omega \tag{3.5}$$

The generalization of Fick's law for three-dimensional diffusion flow is:

$$\boldsymbol{q} = -\boldsymbol{D}\boldsymbol{\nabla} c \tag{3.6}$$

Where $\boldsymbol{q}$ is the chloride ion flux and has dimensions of [kg m^{-2} s^{-1}]. $\boldsymbol{D}$ is the diffusion tensor and has unit of [m^2 s^{-1}] and c is chloride ion concentration [kg m^{-3}].

Using the chain rule $\partial\rho_H/\partial t$ can be derived as:

$$\frac{\partial \rho_H}{\partial t} = \frac{\partial \rho_H}{\partial c} \times \frac{\partial c}{\partial t} = \Phi \frac{\partial c}{\partial t} \tag{3.7}$$

The storage capacity, Φ, is a material parameter and it is unitless [$-$]. Equation (3.5) should hold for any choice of volume Ω and therefore it should be satisfied pointwise. Equations (3.5) and (3.7) are combined together. Therefore,

$$\Phi \frac{\partial c}{\partial t} + div(\boldsymbol{q}) = 0 \tag{3.8}$$

By considering the convective boundary condition, the strong formulation of the transient diffusion becomes:

$$\begin{aligned} \Phi \frac{\partial c}{\partial t} + div(\boldsymbol{q}) &= 0 && \text{in} \quad \Omega \quad \text{for} \quad t \in (0, t_{\text{end}}) \\ q_n &= \alpha(c - c_\infty) && \text{on} \quad \Gamma_c \quad \text{for} \quad t \in (0, t_{\text{end}}) \\ c(x, y, z, 0) &= c_0(x, y, z) && \text{Initial Condition} \end{aligned} \tag{3.9}$$

Following the procedure in Ottosen and Petersson (1992), Equation (3.9) is multiplied by test function, v, and it is integrated over the domain Ω. Thus,

$$\int_{\Omega} v\Phi\frac{\partial c}{\partial t}d\Omega + \int_{\Omega} v\text{div}(\boldsymbol{q})d\Omega = 0 \tag{3.10}$$

The Green-Gauss formula for obtaining the variational(weak) form of the Equation (3.10) is:

$$\int_{\Omega} v\text{div}(\boldsymbol{q})d\Omega = \int_{\Gamma} v\boldsymbol{q}^T\boldsymbol{n}d\Gamma - \int_{\Omega}(\boldsymbol{\nabla}v)^T\boldsymbol{q}d\Omega \tag{3.11}$$

Equation (3.35) is inserted into Equation (3.10) and it is obtained:

$$\int_{\Omega} v\frac{\partial c}{\partial t}d\Omega + \int_{\Omega}(\nabla v)^T(-\boldsymbol{q})d\Omega = -\int_{\Gamma} vq_n d\Gamma \tag{3.12}$$

By introducing the convective boundary condition inside Equation (3.12), the weak form of the transient case is obtained as:

$$\int_{\Omega} v\frac{\partial c}{\partial t}d\Omega + \int_{\Omega}(\nabla v)^T(-\boldsymbol{q})d\Omega = -\int_{\Gamma} v\alpha(c - c_{\infty})d\Gamma \tag{3.13}$$

3.4.2 Finite Element formulation

The finite element method is applied to discretize the system. Therefore, the following approximation is introduced:

$$c \approx c_h = \sum_{i=1}^{\text{Ndof}} N_i a_i = \boldsymbol{N}(\underline{\chi})\boldsymbol{a}(t) \qquad \underline{\chi} = \begin{bmatrix} x \\ y \\ z \end{bmatrix} \tag{3.14}$$

Where $\boldsymbol{N} = [N_1, N_2, \dots, N_{\text{Ndof}}]$ are the element shape functions and $\boldsymbol{a}^T = [a_1, a_2, \dots, a_{\text{Ndof}}]$ are ions concentration at the nodal points. "Ndof" is the total number of degrees of freedom and it is considered before the introduction of boundary conditions.

The approximation of the chloride ions gradient becomes:

$$\boldsymbol{\nabla}c \approx \boldsymbol{\nabla}c_h = \boldsymbol{\nabla}\boldsymbol{N}\boldsymbol{a} = \boldsymbol{B}\boldsymbol{a}; \qquad \text{with} \quad \boldsymbol{B} = \boldsymbol{\nabla}\boldsymbol{N} = \begin{bmatrix} \frac{\partial N_1}{\partial x} & \frac{\partial N_2}{\partial x} & \cdots & \frac{\partial N_{\text{Ndof}}}{\partial x} \\ \frac{\partial N_1}{\partial y} & \frac{\partial N_2}{\partial y} & \cdots & \frac{\partial N_{\text{Ndof}}}{\partial y} \\ \frac{\partial N_1}{\partial z} & \frac{\partial N_2}{\partial z} & \cdots & \frac{\partial N_{\text{Ndof}}}{\partial z} \end{bmatrix} \tag{3.15}$$

The nodal values $\boldsymbol{a}$ are time dependent while the element shape functions are not. Thus:

$$\frac{\partial c}{\partial t} \approx \frac{\partial c_h}{\partial t} = \dot{c}_h = \boldsymbol{N}\dot{a} \tag{3.16}$$

By introducing the approximations, Equations (3.14) to (3.16), into the weak form Equation (3.13):

$$\int_\Omega v\Phi \boldsymbol{N}\dot{a}d\Omega + \int_\Omega (\boldsymbol{\nabla} v)^T(\boldsymbol{D}\boldsymbol{\nabla} c)d\Omega = -\int_\Gamma v\alpha(c - c_\infty)d\Gamma \tag{3.17}$$

The weight functions approximated by the identical element shape functions are introduced using Galerkin's method. Thus,

$$v = \sum_{i=1}^{\text{Ndof}} N_i c_i = \boldsymbol{N}\boldsymbol{c} \tag{3.18}$$

Where $\boldsymbol{c}^T = [c_1, c_2, \dots, c_{\text{Ndof}}]$ are arbitrary coefficients. $\boldsymbol{c}$ is also a scalar, therefore:

$$v = v^T = \boldsymbol{c}^T\boldsymbol{N}^T \tag{3.19}$$

As the same approach in Equation (3.15), it can be written:

$$\boldsymbol{\nabla} v = \boldsymbol{B}\boldsymbol{c} \tag{3.20}$$

Combining Equations (3.18) to (3.20) into Equation (3.17), it is obtained:

$$\int_\Omega \boldsymbol{c}^T\boldsymbol{N}^T\Phi\boldsymbol{N}\dot{a}d\Omega + \int_\Omega \boldsymbol{c}^T\boldsymbol{B}^T(\boldsymbol{D}\boldsymbol{\nabla} c)d\Omega = -\int_\Gamma \boldsymbol{c}^T\boldsymbol{N}^T\alpha(c - c_\infty)d\Gamma \tag{3.21}$$

Equation (3.21) should hold for arbitrary coefficient $\boldsymbol{c}$, Therefore,

$$\boldsymbol{C}\dot{a} + \boldsymbol{K}\boldsymbol{a} = \boldsymbol{f}_b \tag{3.22}$$

Where the matrices and force vector are defined as;

$$\boldsymbol{C} = \int_\Omega \boldsymbol{N}^T\Phi\boldsymbol{N}d\Omega, \qquad \boldsymbol{K} = \int_\Omega \boldsymbol{B}^T\boldsymbol{D}\boldsymbol{B}d\Omega, \qquad \boldsymbol{f}_b = \int_\Gamma \boldsymbol{N}^T\alpha(c - c_\infty)d\Gamma \tag{3.23}$$

Equation (3.22) is expanded as:

$$\boldsymbol{C}\dot{a} + \boldsymbol{K}\boldsymbol{a} = -\int_\Gamma \boldsymbol{N}^T\alpha c d\Gamma + \int_\Gamma \boldsymbol{N}^T\alpha c_\infty d\Gamma \tag{3.24}$$

By implementing Equation (3.14) into Equation (3.24):

$$\boldsymbol{C}\dot{a} + \boldsymbol{K}\boldsymbol{a} = -\left(\int_{\Gamma} \boldsymbol{N}^T \alpha \boldsymbol{N} d\Gamma \right) \boldsymbol{a} + \int_{\Gamma} \boldsymbol{N}^T \alpha c_{\infty} d\Gamma \tag{3.25}$$

Where $\boldsymbol{K}_c$ is defined;

$$\boldsymbol{K}_c = \int_{\Gamma} \boldsymbol{N}^T \alpha \boldsymbol{N} d\Gamma \tag{3.26}$$

Finally, the FE formulation of the transient diffusion is obtained.

$$\boldsymbol{C}\dot{a} + (\boldsymbol{K} + \boldsymbol{K}_c)\boldsymbol{a} = \int_{\Gamma} \boldsymbol{N}^T \alpha c_{\infty} d\Gamma \tag{3.27}$$

Where;

$$\begin{aligned} \boldsymbol{C} &= \int_{\Omega} \boldsymbol{N}^T \Phi \boldsymbol{N} d\Omega \\ \boldsymbol{K} &= \int_{\Omega} \boldsymbol{B}^T \boldsymbol{D} \boldsymbol{B} d\Omega \\ \boldsymbol{K}_c &= \int_{\Gamma} \boldsymbol{N}^T \alpha \boldsymbol{N} d\Gamma \end{aligned} \tag{3.28}$$

3.5 Stationary diffusion FE-formulation

3.5.1 Strong and weak formulations

In this case, a balance or conservation equation is established and the problem is assumed to be time independent. Differential equation of a 3D diffusion problem is:

$$\text{div}(\boldsymbol{D}\boldsymbol{\nabla} c) + Q = 0 \tag{3.29}$$

Where $\boldsymbol{D}$ is diffusion tensor [$m^2\,s^{-1}$], c is chloride ion concentration [$kg\,m^{-3}$] and Q is chloride ion supply [$kg\,m^{-3}\,s^{-1}$].

The generalization of Fick's law for three-dimensional diffusion flow is:

$$\boldsymbol{q} = -\boldsymbol{D}\boldsymbol{\nabla} c \tag{3.30}$$

Where $\boldsymbol{q}$ is the chloride ion flux with the unit of [$kg\,m^{-2}\,s^{-1}$].

Dirichlet(Essential) boundary condition is used to solve the stationary case. Neumann(Natural) boundary condition is not used in this study. The strong form of the stationary case is given by the differential Equation (3.29) together with the boundary conditions, Equation (3.31).

$$\begin{aligned} \operatorname{div}(\boldsymbol{D}\boldsymbol{\nabla} c) + Q = 0 \quad &\text{in} \quad \Omega \\ c = g \quad &\text{on} \quad \Gamma_g \end{aligned} \tag{3.31}$$

Where g is a known quantity. Γ_g is that part of the boundary Γ on which c,the ion concentration is known. Following the procedure in Ottosen and Petersson (1992), Equation (3.29) is multiplied by a test function v and integrated over the entire domain Ω. Hence, it is obtained:

$$\int_\Omega v \operatorname{div}(\boldsymbol{D}\boldsymbol{\nabla}\boldsymbol{c}) d\Omega + \int_\Omega v Q d\Omega = 0 \tag{3.32}$$

By combining Equation (3.30) and Equation (3.32):

$$\int_\Omega v \operatorname{div}(\boldsymbol{q}) d\Omega - \int_\Omega v Q d\Omega = 0 \tag{3.33}$$

The ion supply is considered to be zero since the stationary case is being investigated. Therefore,

$$\int_\Omega v \operatorname{div}(\boldsymbol{q}) d\Omega = 0 \tag{3.34}$$

The Green-Gauss formula for obtaining the variational(weak) form of the Equation (3.34) is:

$$\int_\Omega v \operatorname{div}(\boldsymbol{q}) d\Omega = \int_\Gamma v \boldsymbol{q}^T \boldsymbol{n} d\Gamma - \int_\Omega (\boldsymbol{\nabla} v)^T \boldsymbol{q} d\Omega \tag{3.35}$$

From Equations (3.34) and (3.35):

$$\int_\Omega (\boldsymbol{\nabla} v)^T \boldsymbol{q} d\Omega = \int_\Gamma v \boldsymbol{q}^T \boldsymbol{n} d\Gamma \tag{3.36}$$

Using the boundary condition from Equation (3.31) and by insertion of the constitutive relation Equation (3.30) in Equation (3.36) the following weak from is provided:

$$\begin{aligned} \int_\Omega (\boldsymbol{\nabla} v)^T \boldsymbol{D}\boldsymbol{\nabla} c d\Omega = -\int_{\Gamma_g} v q_n d\Gamma \\ c = g \quad on \quad \Gamma_g \end{aligned} \tag{3.37}$$

3.5.2 Finite Element formulation

The approximation of the ion concentration function is carried out as an interpolation between the nodal points of the elements.

$$c = \boldsymbol{N}\boldsymbol{a} \tag{3.38}$$

where $\boldsymbol{N}$ is the element shape function and $\boldsymbol{a}$ contains the ions concentration at the nodal points. From Equation (3.38) the gradient of the ion concentration becomes:

$$\boldsymbol{\nabla} c = \boldsymbol{B}\boldsymbol{a} \tag{3.39}$$

where the three-dimensional elements imply that:

$$\nabla c = \begin{bmatrix} \dfrac{\partial c}{\partial x} \\ \dfrac{\partial c}{\partial y} \\ \dfrac{\partial c}{\partial z} \end{bmatrix}; \quad \boldsymbol{B} = \begin{bmatrix} \dfrac{\partial N_1}{\partial x} & \dfrac{\partial N_2}{\partial x} & \cdots & \dfrac{\partial N_{\text{Ndof}}}{\partial x} \\ \dfrac{\partial N_1}{\partial y} & \dfrac{\partial N_2}{\partial y} & \cdots & \dfrac{\partial N_{\text{Ndof}}}{\partial y} \\ \dfrac{\partial N_1}{\partial z} & \dfrac{\partial N_2}{\partial z} & \cdots & \dfrac{\partial N_{\text{Ndof}}}{\partial z} \end{bmatrix} \tag{3.40}$$

Equation (3.39) is implemented into Equation (3.37). Hence , results in:

$$\left(\int_{\Omega} (\boldsymbol{\nabla} v)^T \boldsymbol{D}\boldsymbol{B} d\Omega \right) \boldsymbol{a} = - \int_{\Gamma_g} v q_n d\Gamma \tag{3.41}$$

In accordance with the Galerkin method:

$$\begin{aligned} v &= \boldsymbol{N}\boldsymbol{c} \\ v &= \boldsymbol{c}^T \boldsymbol{N}^T \end{aligned} \tag{3.42}$$

The matrix $\boldsymbol{c}$ is arbitrary since v is arbitrary. Therefore, from Equation (3.42) it is obtained:

$$\nabla v = \boldsymbol{B}c \tag{3.43}$$

Equations (3.42) and (3.43) are inserted into Equation (3.41) and therefore results in:

$$\left(\boldsymbol{c}^T \int_{\Omega} \boldsymbol{B}^T \boldsymbol{D}\boldsymbol{B} d\Omega \right) \boldsymbol{a} = -\boldsymbol{c}^T \int_{\Gamma_g} \boldsymbol{N}^T q_n d\Gamma \tag{3.44}$$

$\boldsymbol{c}$ is independent of the position and Equation (3.44) should hold for any arbitrary $\boldsymbol{c}^T$ matrices. The FE formulation of is derived as:

$$\left(\int_{\Omega} \boldsymbol{B}^T \boldsymbol{D} \boldsymbol{B} d\Omega \right) \boldsymbol{a} = - \int_{\Gamma_g} \boldsymbol{N}^T q_n d\Gamma \tag{3.45}$$

where;

$$\begin{aligned} \boldsymbol{K} &= \int_{\Omega} \boldsymbol{B}^T \boldsymbol{D} \boldsymbol{B} d\Omega \\ \boldsymbol{f}_b &= - \int_{\Gamma_g} \boldsymbol{N}^T q_n d\Gamma \end{aligned} \tag{3.46}$$

Finally, the FE form can be written as:

$$\boldsymbol{K} \boldsymbol{a} = \boldsymbol{f}_b \tag{3.47}$$

4 Experimental Procedure

4.1 Introduction

The model combine finite element analysis and material homogenization to determine transport phenomenon in concrete. By using this model, it is required to explore the effects of changing various parameters, e.g. different size of components or varied material properties.

An effort is taken to assess the sensitivity of the model to discover main effects of varied input parameters and possible interaction between them. This is performed by a statistical method, called factorial design.

4.2 Factorial design

In this method, fixed number of "levels"(versions) are assigned to a number of factors(variables) and the experiments are performed in all possible combinations. Box et al. (2005) explains why the Factorial Experiments are preferred to the normal method which factors are varied one at a time with the remaining factors held constant. The Factorial shows the additivity of the factors with much more precision. Furthermore, if the factors do not act additively, the Factorial can detect and estimate interactions that measure the non-additivity.

A simple example of a 2^2-design is going to be explained. Two different levels are assigned to two factors, see Table 4.1.

Table 4.1: *Levels of factors*

Factors	Levels	
	−	+
A	A^-	A^+
B	B^-	B^+

Following the procedure in Box et al. (2005), *the table of contrast* is shown in Table 4.2. The table begins with run numbers followed by two columns **A**, **B** that define the design matrix of the 2^2 factorial design. This is followed by the interaction additional column identified as **AB**. The responses which are treated as single observations, are shown in the last column of the table.

Table 4.2: *Table of contrast coefficient for a* 2^2 *factorial design*

Run #	A	B	AB	Response, y
1	−	−	+	y_1
2	+	−	−	y_2
3	−	+	−	y_3
4	+	+	+	y_4

The main and interaction effects of the factors can be calculated following a matrix notation. Thus,

$$\boldsymbol{E} = \frac{2}{n_{\text{runs}}} \underbrace{\begin{bmatrix} -1 & +1 & -1 & +1 \\ -1 & -1 & +1 & +1 \\ +1 & -1 & -1 & +1 \end{bmatrix}}_{\boldsymbol{C}_{\boldsymbol{M}}^{T}} \underbrace{\begin{bmatrix} y_1 \\ y_2 \\ y_3 \\ y_4 \end{bmatrix}}_{\boldsymbol{R}} = \begin{bmatrix} \boldsymbol{A}_{\text{main.}} \\ \boldsymbol{B}_{\text{main.}} \\ \boldsymbol{AB}_{\text{int.}} \end{bmatrix} \tag{4.1}$$

Where:

$$\boldsymbol{C_M} = \text{contrast matrix} = \begin{bmatrix} -1 & -1 & +1 \\ +1 & -1 & -1 \\ -1 & +1 & -1 \\ +1 & +1 & +1 \end{bmatrix}$$

$\boldsymbol{R}$ = response vector
$\boldsymbol{E}$ = vector of effects
n_{runs} = total number of runs/simulations

4.2.1 Scope of relevant work using factorial design

Dar et al. (2002) performed factorial and probabilistic analyses on a finite element model of a beam. The intention of the study was to minimize the generated stress in the beam by adjusting the geometrical and material properties within a prescribed range. They performed different levels of factorial analyses, e.g.

two-level full factorial design and three-level fractional factorial design. Finally, four-level fractional factorial was performed only considering the main effects, not interactions. The four-level fractional factorial resulted in the same answers for only half the experimental effort of the other designs. Despite the huge saving in time, the interactions could not be measured in the four-level fractional factorial. Furthermore, the most important factors and sensitivity of the parameters were identified.

In a clinical research carried out by Petrie and Williams (2005), 3D finite element models of premolar mandible with an embedded implant inside cancellous bone were generated. A two-level factorial design was utilized to investigate crestal bone strains. This resulted in the most favourable choice in order to minimize the implant strain in the crestal bone.

4.3 Fractional factorial design

In a fractional factorial design, information on the main effects and low-order interactions are obtained by running only a fraction of the complete factorial experiment. According to Montgomery (2009), the experimenter can assume that certain high-order interactions are negligible. Therefore, this method is useful while many factors are considered and the objective is to find out if those factors have large or little or no effect on the response. Saltelli et al. (2008) claims that when the number of parameters is large, the number of *influential* parameters is *always* small. The inefficiency of the one-at-a-time sampling is also true in this case. In fact, if only a few parameters are influential, then most of the simulations would be devoted to determining the very small effects of noninfluential parameters.

4.3.1 Scope of relevant work using fractional factorial design

Parghi and Alam (2016) studied the effects of seven parameters concerning seismic behaviour of reinforced concrete bridge piers confined with Fibre Reinforced Polymer(FRP). The geometry of the bridge was modelled as a 2D finite element frame and the results from the model were validated with experimental results. A seven factor with three-level fractional factorial design was performed. The effect of individual factors and their interactions on the limit states of the confined FRP bridge piers were investigated. They observed height-to-depth ratio of column is the most important factor. Moreover, a significant effect of longitudinal steel reinforcement on the yield and base shear of the confined FRP piers was noticed.

5 Results

5.1 Stationary Case Investigation

5.1.1 Mesh convergence study

A Number of runs on a SVE with the size of 4 cm with increasing levels of mesh refinement are used to illustrate mesh convergence. As the mesh gets finer, the result of the simulations become more accurate. The model consists of three phases i.e., cement, ballast and ITZ. Choosing a finer mesh leads to formation of a decent SVE as it is presented in Figure 5.1.

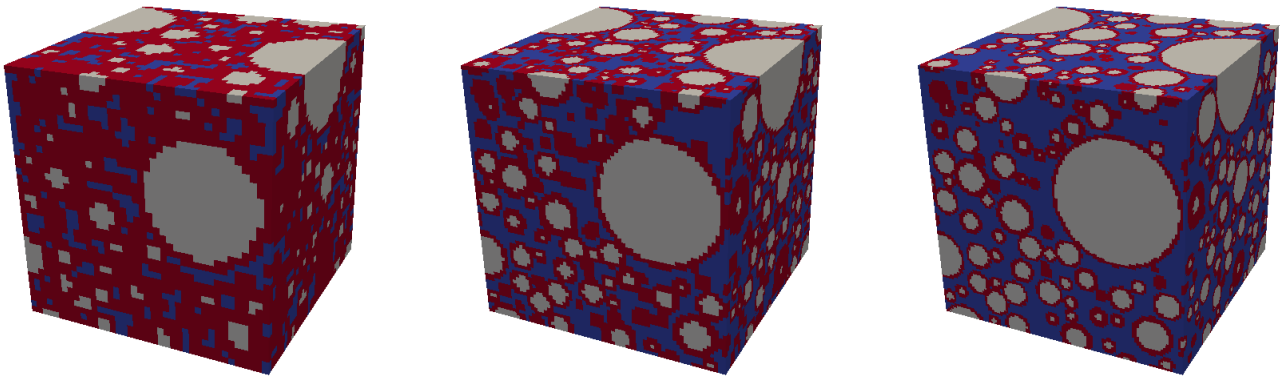

(a) $nx = 40$ (b) $nx = 70$ (c) $nx = 110$

Figure 5.1: *Visualiztion of different mesh sizes. The grey color represent ballast, blue represent cement and red reoresent ITZ.*

The mesh convergence study is carried out on diagonal components of diffusivity tensor, Figure 5.2a. The normalized error is presented in Figure 5.2b using the function developed by Johansson (2011). Diagonal components of diffusivity tensor are compared in order to select a proper mesh size. Finally, mesh size 100 was chosen for a SVE with the size of 4 cm which represent 100^3 Number of Elements (NEL) within the whole SVE.

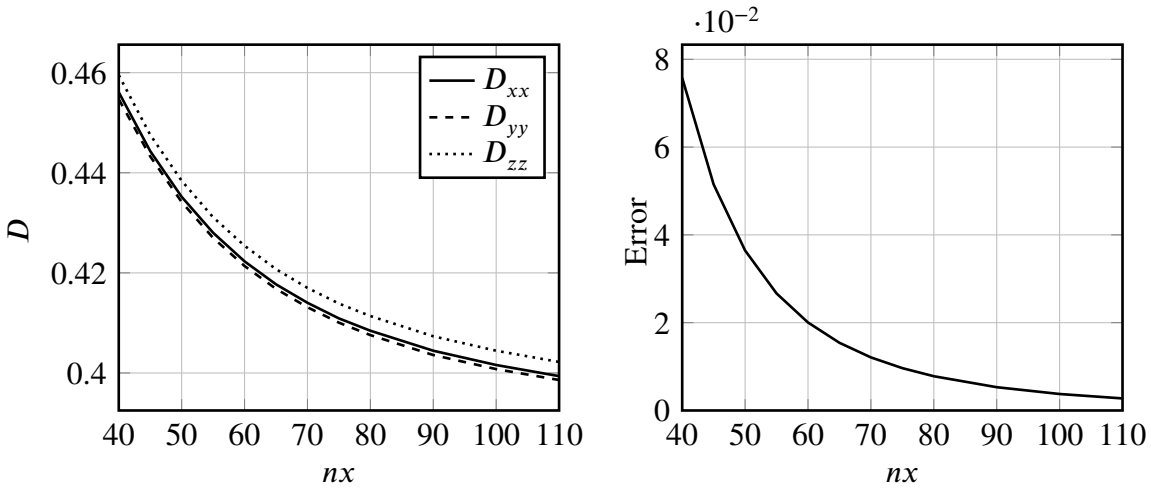

(a) *Mesh convergence study* (b) *Normalized error*

Figure 5.2: *Stationary diffusion mesh convergence study for a SVE with the size of 4 cm.*

5.1.2 Two-level factorial design

The statistical work in this thesis started by considering two levels for each factor in order to determine a promising direction for further experimentation. Two-level factorial design needs rather few runs per

factor studied and the results can be obtained using basic arithmetic (Box et al., 2005). All the graphs relating to factorial design of this study are generated using MATLAB (2017).

5.1.2.1 Experimental procedure

The experiment employed a 2^3 factorial experimental design with three quantitative factors. Two levels are assigned to each factors meaning that a two-level factorial design has performed. The factors are presented in Table 5.1 with the corresponding minimum and maximum levels.

Table 5.1: *Levels of factors*

	Factor levels	−	+
A	Gravel Content [%]	10	40
B	Size of SVE [cm]	2	4
C	ITZ diffusivity [-]	0.00	0.15

The components of the diffusivity tensor is as Equation (3.1). Each data value saved, is for the response diffusivity tensor and run time which corresponds to solving the linear stationary formulation. Therefore, six components of the diffusivity tensor, Equation (3.1), and the run time are evaluated. Each run is replicated three times and the average of the corresponding responses are calculated. Table 5.2 shows the combinations of the coded factor levels.

Table 5.2: *A* 2^3 *factorial fesign: combinations of the factors*

Run #	**A**	**B**	**C**
1	−	−	−
2	+	−	−
3	−	+	−
4	+	+	−
5	−	−	+
6	+	−	+
7	−	+	+
8	+	+	+

5.1.2.2 Results

The estimated main effects of the factors are presented in Figure 5.3. D_{xx} diffusivity component decreases as the gravel content level increases. Aggregates behave like a barrier to the transportation of the moisture or chloride since they are assumed to be impermeable; therefore, the diffusivity of concrete decreases. Changing the size of the SVE should not result in diffusion differences. However, the difference is quite large in this two-level experiment. This demands a size investigation study in order to find the proper SVE size, see Section 5.1.3. The ITZ diffusivity factor has the largest effect among the others. By increasing the amplitude of this factor, D_{xx} increases. In general, ITZ diffusivity plays an important role

in diffusion process since it is a highly diffusive interface.

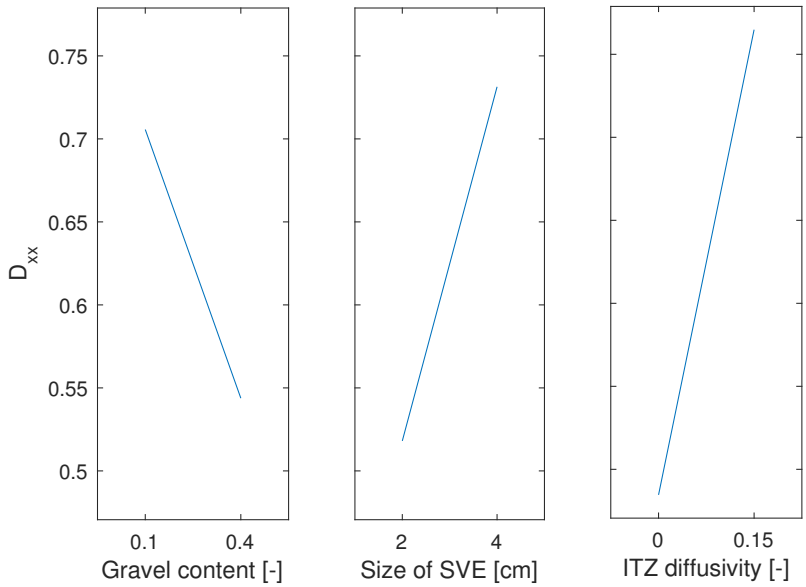

Figure 5.3: *Main effects of two-level factorial design. The vertical axis shows the average of diffusivity component,* D_{xx}.

5.1.3 Scale effect(size investigation)

As it was described in Section 5.1.2.2, the proper size of the SVE should be investigated due to the significant difference of the main components of diffusion tensor.

5.1.3.1 Experimental procedure

For this experiment, new SVEs are only created for the new size level combinations. Therefore, the previous responses from Section 5.1.2.2 are conserved and only the new combinations are simulated. Six different levels of SVE sizes are assigned to perform a multi-level experimentation, see Table 5.3. All the components of diffusivity tensor, Equation (3.1), are used as the response. The model locate the aggregates randomly within the SVE. In order to reduce the standard error of a particular effect, each of the eight responses is the average of the three genuinely replicated runs shown in Table 5.3.

It should be noted that, as the size of the SVE increases, the mesh size needs to get finer. Therefore, a linear relation from Section 5.1.1 is used to increase the number of elements with respect to size of the SVE, Equation (5.1). In Equation (5.1), *nx* represents the number of elements along each side of SVE and $L_{\square}$ is the side length of the SVE in [cm].

$$nx = 15L_{\square} + 40 \tag{5.1}$$

Table 5.3: *Size investigation: Levels of factors*

	Factor levels	1	2	3	4	5	6
A	Gravel Content [%]	10	40				
B	Size of SVE [cm]	2	4	6	8	10	12
C	ITZ diffusivity [-]	0.00	0.15				

5.1.3.2 Results

The results of the scale effect is presented in Figure 5.4. The diffusion component decreases non-linearly as the the size of the SVE increases. Furthermore, the diffusion reduction rate, decreases in larger sizes. The computational run time analysis on Cluster[†] are shown in Figure 5.5. There is a huge difference between the sensitivity of changing the size of SVE compare to gravel content and ITZ diffusivity. Therefore, 8 cm SVE is used as the decent size considering run time of the simulations to perform further experimentation.

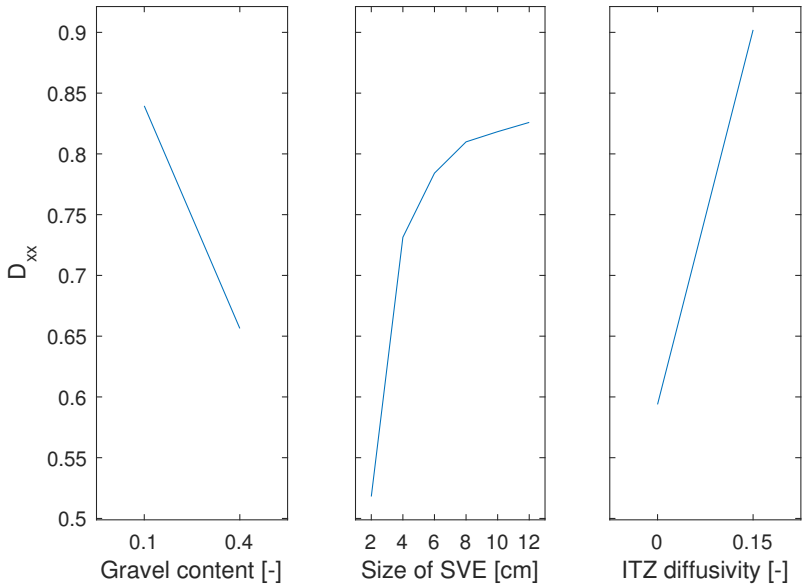

Figure 5.4: *Main effects of multi-level factorial design regarding the size investigation. The vertical axis shows the average of diffusivity component,* D_{xx}.

[†]Cluster Hebbe is used on C3SE resources. The documentation of C3SE can be found on: `http://www.c3se.chalmers.se/index.php/Main_Page`

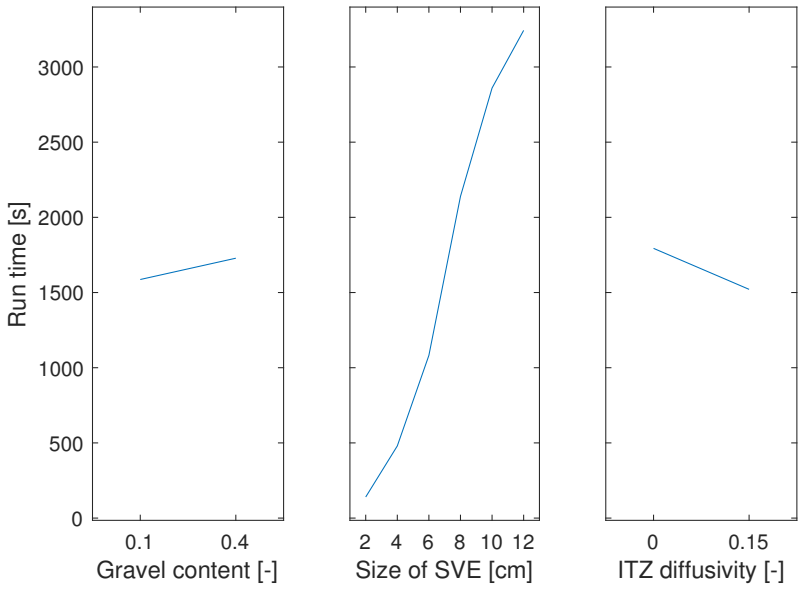

Figure 5.5: *Run time measured in seconds in order to solve the nodal values in stationary diffusion. The vertical axis shows the average measured time in seconds.*

5.1.4 Gravel content and ITZ diffusivity behaviour

After choosing the proper SVE size, the behaviour of the other two factors, i.e gravel content and ITZ diffusivity are put to discussion.

5.1.4.1 Experimental procedure

More number of levels are assigned to these two factors utilizing a SVE with the size of 8 cm. The levels are shown in Table 5.4.

Table 5.4: *Size investigation: Levels of factors*

	Factor levels	1	2	3	4
A	Gravel Content [%]	10	25	40	50
B	ITZ diffusivity [-]	0.00	0.075	0.15	0.25

5.1.4.2 Results

The two factors studied behave quite linearly as it is presented in Figure 5.6. Moreover, The effect of ITZ diffusivity factor is more compare to the aggregate content. The interaction between the these two factors is another aspect which is investigated.

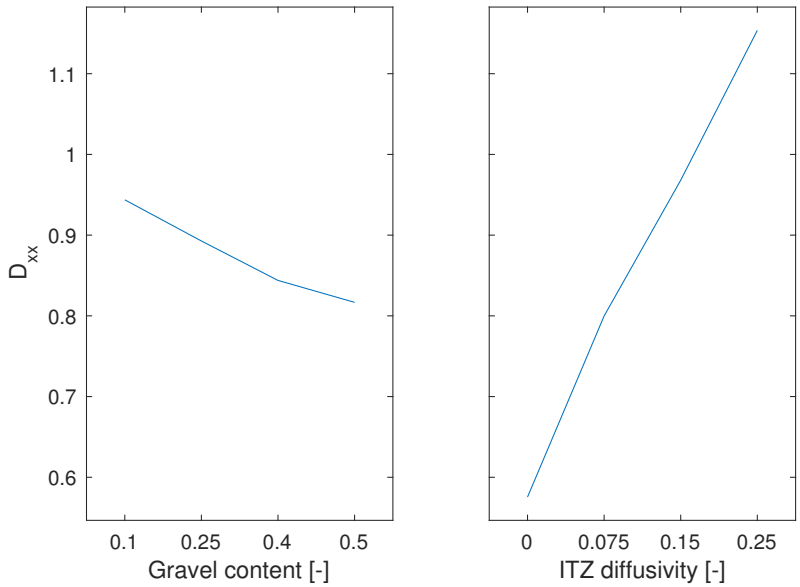

Figure 5.6: *Main effects of multi-level factorial design. The vertical axis shows the average of diffusivity component,* D_{xx}.

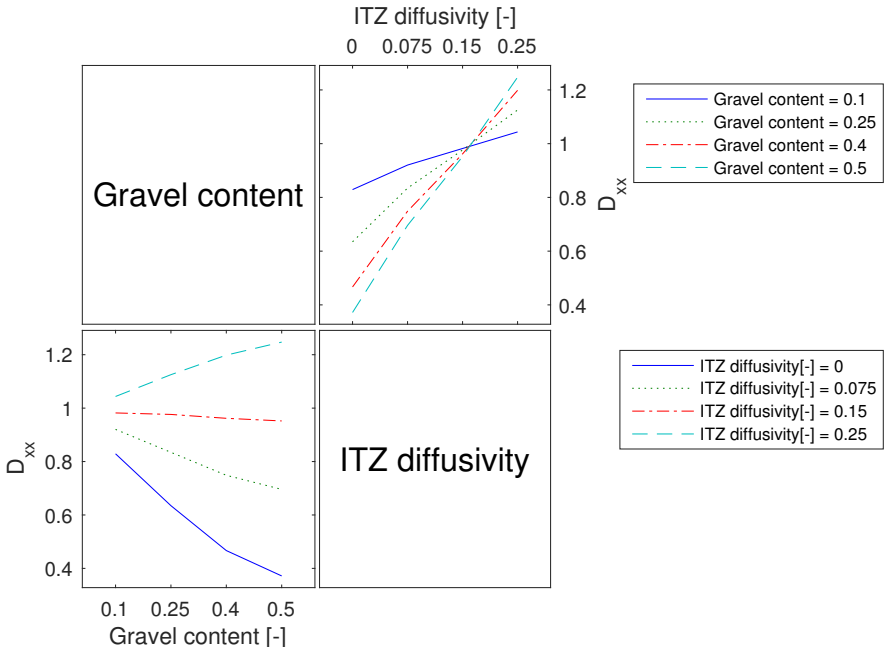

Figure 5.7: *Interaction plot of gravel content and diffusivity of ITZ. The vertical axis of both graphs shows the average of diffusivity component,* D_{xx}.

The upper right graph in Figure 5.7 explains the ITZ diffusivity raise with respect to different gravel contents. The difference in diffusion for lower amount of aggregate is low. However, as the amount of aggregate increases, the difference becomes higher so does the slope of them. This behaviour has a

physical explanation. By increasing number of aggregates in a mix design of concrete, the surface area of the interfacial zone increases. The ITZ has a porous and diffusive property; Therefore, reinforced concrete with higher proportion of aggregates can have detrimental impact on the reinforcements in terms of chloride ingress. The lower left corner graph is explaining a similar pattern. However, the order of factors is the opposite.

5.2 Transient Case Investigation

Concrete cover is one of the durability requirements in the design of reinforced concrete structures. EN-1992-1-1 (2004) defines the nominal concrete cover as:

$$C_{\text{nom}} = C_{\text{min}} + \Delta C_{\text{dev}} \tag{5.2}$$

Where C_{min} is the minimum concrete cover, ΔC_{dev} is the allowed concrete cover deviation in design. The minimum cover is calculated as:

$$C_{\text{min}} = \max\{C_{\text{min,b}}; C_{\text{min,dur}} + \Delta C_{\text{dur},\gamma} - \Delta C_{\text{dur,st}} - \Delta C_{\text{dur,add}}; 10(\text{mm})\} \tag{5.3}$$

Where:

$C_{\text{min,b}}$	=	minimum cover due to bond requirement
$C_{\text{min,dur}}$	=	minimum cover due to environmental conditions
$\Delta C_{\text{dur},\gamma}$	=	additive safety element
$\Delta C_{\text{dur,st}}$	=	reduction of minimum cover for use of stainless steel
$\Delta C_{\text{dur,add}}$	=	reduction of minimum cover for use of additional protection

Since chloride ingress is examined; therefore, the recommended cover due to environmental conditions is used. The smallest concrete cover due to corrosion induced by chlorides, XD1/XS1 is 20 mm. XD1 is the corrosion induced by chlorides in moderate humidity. XS1 is the corrosion induced by chloride from sea water for members exposed to airborne salt but not in direct contact with sea water (EN-1992-1-1, 2004).

In this study 20 mm concrete is used for the transient simulations. A function is implemented in order to extract the nodal values which corresponds to 20 mm from the surface of the SVE, see Figure 5.8.

5.2.1 Time step convergence study

A variety of time step and step sizes can be used in the transient model. The nodal values are solved in each time step and the multiplication of the time step and step size results in the total time. A time convergence study is significant in order to find a decent time step.

Three different time steps and step size are performed. All the alternatives evaluate total of 10 years. However, as the step size decreases, the solved nodal values becomes more accurate. Table 5.5 shows the results with different time steps in terms of run time on the Cluster to solve the transient diffusion.

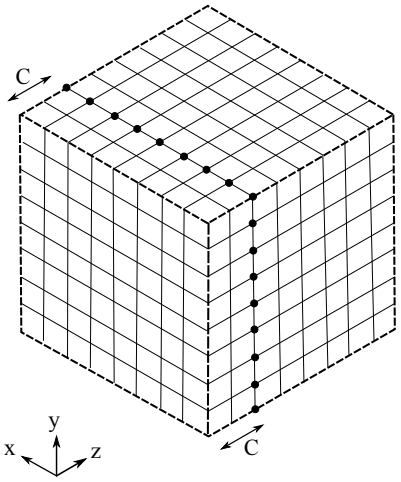

Figure 5.8: *Nodes corresponds to chosen concrete cover in z-direction.*

Table 5.5: *Run time to solve the transient nodal values*

#	Time step	step size	Total time	Run time h:min:s	Average iteration to converge to solution	Residual
1	10	1	10	3 : 16 : 03	164	10^{-6}
2	20	0.5	10	3 : 58 : 05	118	9.8×10^{-7}
3	40	0.25	10	3 : 21 : 02	84	9.9×10^{-7}

All the nodal values on 2 cm plane from the nearest concrete surface are evaluated. Vertical axis of Figure 5.9 shows the maximum difference between nodal value and chloride initial condition. As it can be seen the curve for time steps 20 and 40 are closer together compare to time steps 10 and 20. By decreasing the step sizes, the nodal value limits to an accurate value.

Finally, time step 40 with steps size 0.25 is chosen for further experimentations by comparing the run time and accuracy presented in Table 5.5 and Figure 5.9.

5.2.2 Boundary condition and choice of SVE

Consider a reinforced concrete beam which is exposed to chloride environment. The SVE in this investigation, represent 8 cm cube which is assumed to be cut out from this concrete beam, see Figure 5.10a. With this assumption, five sides of the concrete cube will be isolated and only one side is exposed to ambient chloride, see Figure 5.10b.

5.2.3 Fractional factorial design

In sequential experimentation, it is usually the best to start with a fractional factorial design. In other words, the first fractional design will indicate how a further fraction should be chosen. This can lead to a larger design to answer questions and resolve the ambiguities (Box et al., 2005).

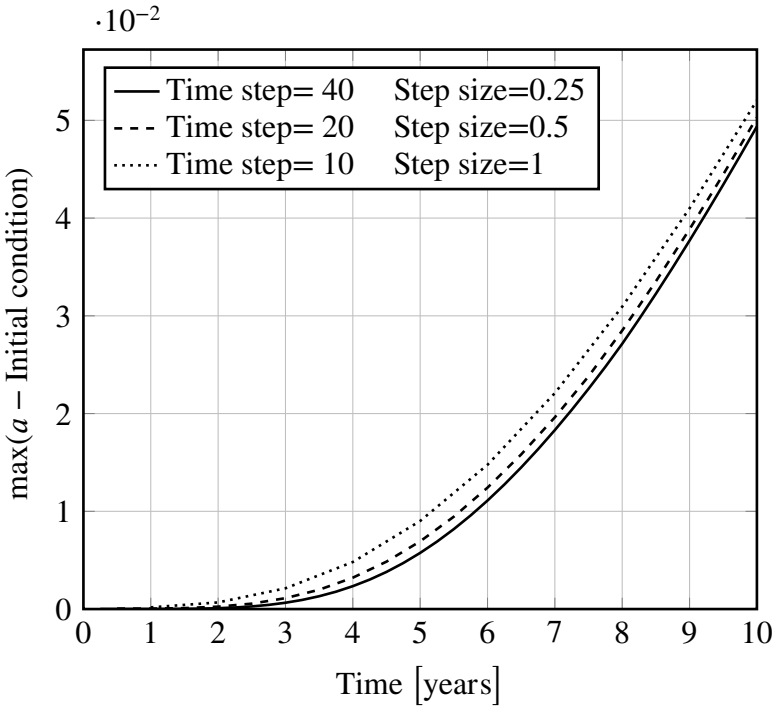

Figure 5.9: *Time convergence study for transient diffusion.*

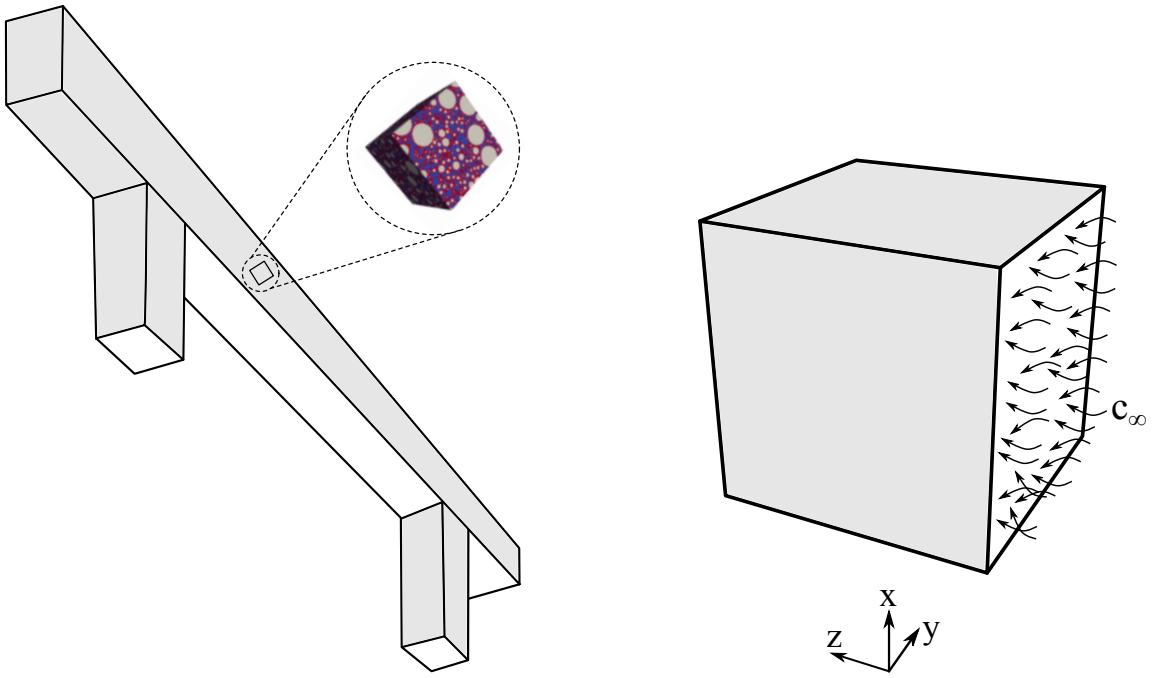

Figure 5.10: (*a*) *Reinforced concrete beam exposed to chloride including the SVE taken from side of the beam.* (*b*) *Choice of boundary conditions for the SVE. The gray sides are not exposed to ambient chloride.*

5.2.3.1 Experimental procedure

In table Table 5.6, input parameters of six factors, lower and higher levels for performing the fractional factorial sampling are presented. The lower and upper levels changed with a relative amount. The minimum level is decreased 5 % while the maximum is increased by 5 %. A $2^{6-2}_{\mathbf{IV}}$ fractional factorial design is performed. The resolution of the design is considered to be **IV** because usually three-factor interactions can be assumed to be negligible.

Table 5.6: *Levels of factors*

	Description	Factors	Unit	Chosen value	−	+
A	Gravel Content	n_b	[-]	0.4	0.38	0.42
B	Cement storage capacity	Φ	[-]	10	9.5	10.5
C	Cement diffusivity	D_{cp}	$\mathrm{cm}^2\ \mathrm{year}^{-1}$	0.55	0.52	0.58
D	Convective coefficient	α	$\mathrm{cm\ year}^{-1}$	200	190	210
E	Ambient chloride	c_∞	$\mathrm{g\ cm}^{-3}$	1.00	0.95	1.05
F	ITZ diffusivity	D_{ITZ}	$\mathrm{cm}^2\ \mathrm{year}^{-1}$	0.01	0.0095	0.0105

Table 5.7: *Fractional factorial design: Levels of factors and the respone*

	a	**b**	**c**	**d**	**bcd**	**acd**	**Response**
Test #	**A,** n_b	**B,** Φ	**C,** D_{cp}	**D,** α	**E,** c_∞	**F,** D_{ITZ}	t, year
1	−	−	−	−	−	−	5.75
2	−	−	−	+	+	+	5.50
3	−	−	+	−	+	+	5.00
4	−	−	+	+	−	−	5.25
5	−	+	−	−	+	−	4.972
6	−	+	−	+	−	+	6.25
7	−	+	+	−	−	+	5.75
8	−	+	+	+	+	−	5.75
9	+	−	−	−	−	+	6.00
10	+	−	−	+	+	−	6.00
11	+	−	+	−	+	−	5.50
12	+	−	+	+	−	+	5.50
13	+	+	−	−	+	+	6.50
14	+	+	−	+	−	−	6.75
15	+	+	+	−	−	−	6.25
16	+	+	+	+	+	+	6.00

Simulations are investigated for total time of ten years. The goal is to capture the time which the chloride exceeds one percent of the initial chloride condition. Thus, when the difference of nodal values, $\boldsymbol{a}$, and the chloride initial condition reaches beyond one percent, the time step is reported. The results are

shown in Table 5.7, which t is the time which nodal values located at cover size exceeds by one percent of initial chloride condition.

5.2.3.2 Results

The main effects of the six factors from the fractional factorial design are shown in Figure 5.11. It is observed that the gravel content has a dominant effect among the other parameters. When concrete has more aggregates, it takes longer time for the chloride ions to dodge the aggregates since aggregate is not a diffusive material.

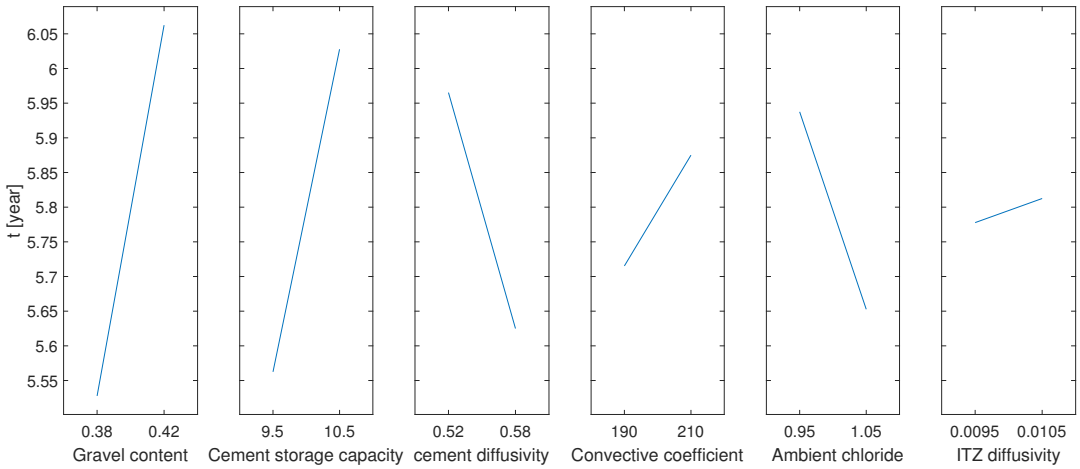

Figure 5.11: *Result of the* $2^{6-2}_{\mathbf{IV}}$ *fractional factorial design. The vertical axis shows the response,t, in year.*

Cement storage capacity has the second largest effect. When chloride ions enter a material, portion of them are bound with the material. Therefore, for a concrete with higher cement storage capacity, it takes longer time to reach the chloride concentration threshold at the cover. The third dominant factor is the cement diffusivity. The raise in cement diffusivity results in reduction of the response since more chloride ions will travel through the surface in time.

Convective coefficient relates to the roughness of the concrete surface. Chlorides have harder time to penetrate into a SVE with higher convective coefficient. It takes less amount of time for the chlorides to reach the chloride threshold and the negative slope of the ambient chloride explains this. Finally, ITZ diffusivity has almost a negligible effect. It is worth to mention, ITZ diffusivity was a dominant factor in the stationary investigations which is not in transient study. Therefore, it is important to evaluate both stationary and transient cases, otherwise a wrong conclusion may be jumped in.

5.2.4 Full factorial design

The motivation of performing Section 5.2.3 was to screen for important factors. Hence, three factors showing higher effects are considered to perform a full factorial design in order to find the possible interactions between them. The screened factors are: gravel content, cement diffusivity and cement storage capacity.

5.2.4.1 Experimental procedure

A 2^3 factorial experimental design is employed with three quantitative factors. The variable levels are assigned according to Table 5.8. The value for the screened out factors - convective coefficient, ambient chloride and ITZ diffusivity - are chosen as the middle value of the Table 5.6. The initial chloride condition is 0.005 g cm^{-3}.

Table 5.8: *Full factorial design: levels of factors*

	Description	Factors	Unit	Chosen value	−	+
A	Cement diffusivity	D_{cp}	cm^2 year^{-1}	0.55	0.52	0.58
B	Cement storage capacity	Φ	[-]	10	9.5	10.5
C	Gravel content	n_b	[-]	0.4	0.38	0.42

The measured response is the time corresponding to one percent exceeder of chloride ions at concrete cover. The simulation runs with the calculated responses are shown in Table 5.9.

Table 5.9: *Full factorial design: Levels of factors and the respone*

Test #	A, D_{cp}	B, Φ	C, n_b	Response, t, year
1	−	−	−	5.75
2	+	−	−	5.25
3	−	+	−	6.25
4	+	+	−	5.75
5	−	−	+	6.00
6	+	−	+	5.50
7	−	+	+	6.75
8	+	+	+	6.00

5.2.4.2 Results

Raising the cement diffusivity cuts the time by about 10 percent. An Increase in cement storage capacity by the same amount, results in the same enlargement of time. Increasing the gravel content has half effect of the others. The study of main effects are presented in Figure 5.12.

By comparing the results from the Sections 5.2.3.2 and 5.2.4.2, the gravel content has a different effect magnitude. In fractional factorial with resolution **IV**, main effects are only aliased with three-factor interaction. Therefore, higher order interactions influence the gravel content in Section 5.2.3.2. In general, results from full factorial sampling is more accurate since no main effects are aliased with other main effects or factor interactions.

The interactions of the factors are shown in Figure 5.13. The parameters appear to be substantially free of interactions since the lines are parallel. Observing no interactions between the gravel content and the other two parameters is reasonable since there are no logical relations between the cement and aggregates in the model. There is also a mathematical explanation for absence of interaction between the

cement storage capacity and its diffusivity. According to Equations (3.27) and (3.28), storage capacity and diffusivity exist in two different terms. Thus, no interaction should be expected between these two parameters. However, this should be called into question in experimental designs to observe the existence of interaction between diffusivity of cement and storage capacity.

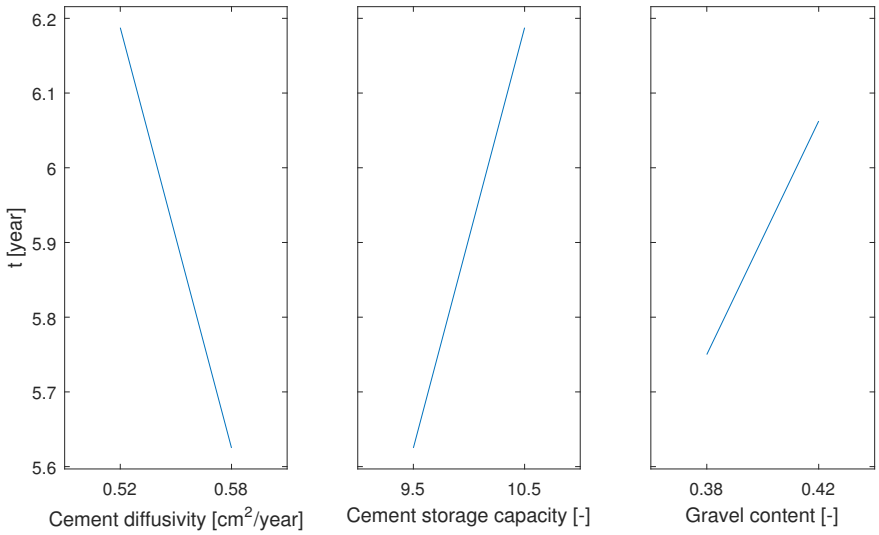

Figure 5.12: *Result of the 2^3 full factorial design. The vertical axis shows the response,t, in year.*

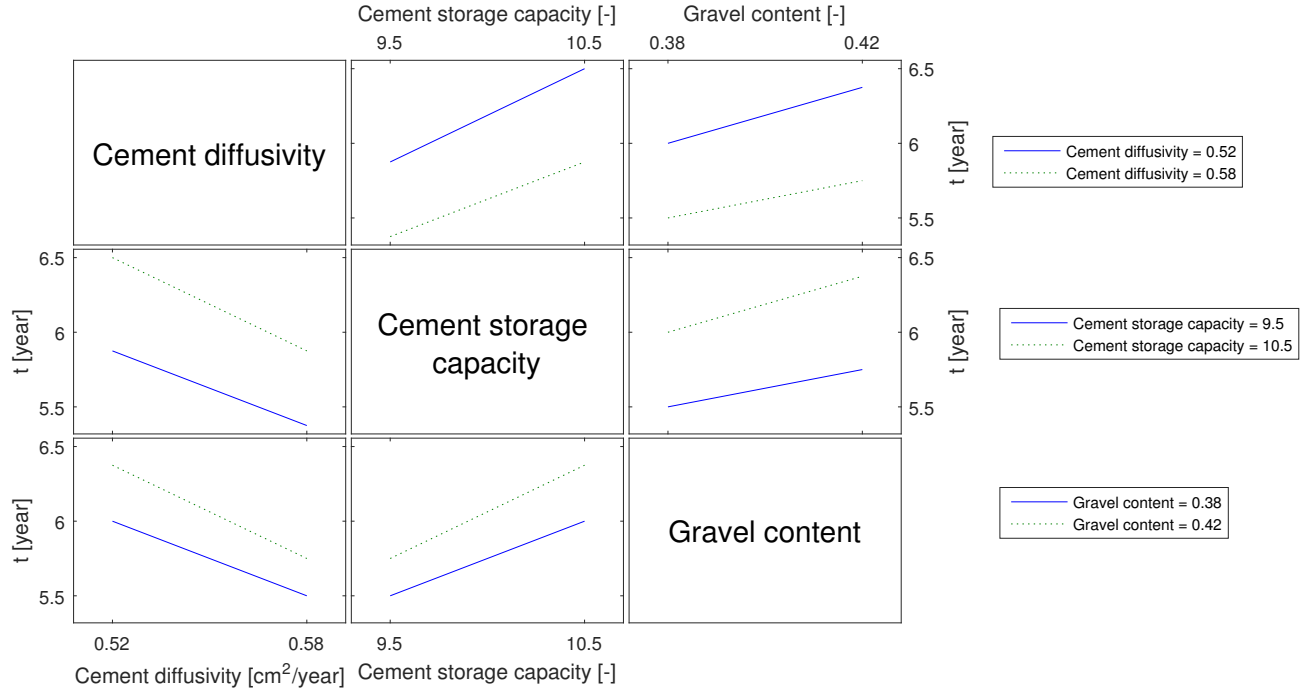

Figure 5.13: *Interactions between the chosen factors in transient study. The vertical axis shows the response,t, in year.*

6 Conclusions and outlook

6.1 General conclusions

The goal of this work was to evaluate transport of chloride ions in concrete using a 3D finite element heterogeneous model. This goal was achieved by carrying out factorial design following the examination of the stationary and transient model responses.

In the stationary case, it was observed that the diagonal components of the diffusion tensor decreases non-linearly with increasing the size of the SVE. However, aggregate content and diffusivity of ITZ are behaving quite linearly while diffusivity of ITZ is more sensitive. There is also an interaction between the aggregate content and ITZ diffusivity. The interaction shows corrosion deterioration can facilitate in reinforced concrete with higher proportion of aggregates and ITZ diffusivity.

The results obtained from the transient study show that the aggregate content has a dominant effect. Thus, gravel content is a matter of some concern to set up the experiments. Two other significant factors are cement storage capacity and diffusivity of cement. Additionally, in contrast to stationary investigation, ITZ diffusivity has a minor effect. Calculating the diffusivity of ITZ in experiments is a matter of concern. Having in mind transient case represent the diffusion closer to reality, due to the slight effect, ITZ diffusivity can be neglected for future experimental studies.

The full factorial design on screened parameters- gravel content, cement storage capacity and cement diffusivity- shows a difference between the effect of gravel content in fractional and full factorial study due to higher order interactions in fractional resolution **IV**. Moreover, this closer investigation shows no interactions between the studied factors.

In general, the factorial design method provide an efficient evaluation of the model. The statistical results shows the model, behaves corresponding to the utilised mathematical formulations.

6.2 Suggestion for future research

In order to give realistic predictions of chloride ingress in concrete, a proper calibration with experimental data is crucial. The experiments should be set up close to the characteristics of the model in respect of dimensions of the factors and general assumptions. There are also some parameters that needs to be determined according to experiments, e.g. storage capacity, convective coefficient and ITZ diffusivity of concrete.

Finally, an identical factorial design can be carried out on experimental studies for further validation and calibration of the model with real phenomenon.

References

EN-1992-1-1 (2004). *Eurocode2: Design of concrete structures - Part 1-1: General rules and rules for buildings*. EUROPEAN COMMITTEE FOR STANDARDIZATION (cit. on p. 23).

Ababneh, A. and Y. Xi (2002). "An experimental study on the effect of chloride penetration on moisture diffusion in concrete". In: *Material and Structures* 35.254, pp. 659–663. ISSN: 1359-5997. DOI: 10.1617/13936 (cit. on pp. 4, 7).

Blomfors, M., D. Coronelli, K. Lundgren, and K. Zandi (2017). "Engineering bond model for corroded reinforcement". In: *Engineering Structures*. Submitted (cit. on p. 1).

Box, G. E., J. S. Hunter, and W. G. Hunter (2005). *Statistics for Experimenters*. 2nd ed. Hoboken, New Jersey: John Wiley and sons, p. 664. ISBN: 978-0-471-71813-0 (cit. on pp. 14, 15, 18, 24).

Černý, R. and P. Rovnaníková (2002). *Transport Processes in Concrete*. London: Spon Press, p. 547. ISBN: 0-415-24264-9 (cit. on p. 3).

Dar, F. H., J. R. Meakin, and R. M. Aspden (2002). "Statistical methods in finite element analysis". In: *Journal of Biomechanics* 35.9, pp. 1155–1161. ISSN: 00219290. DOI: 10.1016/S0021-9290(02)00085-4. URL: http://linkinghub.elsevier.com/retrieve/pii/S0021929002000854 (cit. on p. 15).

Eckerdal, A. (2006). "Novice Students' Learning of Object-Oriented Programming." IT Licentiate of Philosophy thesis in Computer Science. Licentiate thesis. Uppsala University: Department of Information Technology (cit. on p. 4).

Eckerdal, A. and M. Thuné (2005). "Novice Java programmers' conceptions of "object" and "class", and variation theory". In: *Proceedings of the 10th annual SIGCSE conference on Innovation and technology in computer science education - ITiCSE '05*. New York, New York, USA: ACM Press, p. 89. ISBN: 1595930248. DOI: 10.1145/1067445.1067473. URL: http://portal.acm.org/citation.cfm?doid=1067445.1067473 (cit. on p. 4).

Homan, L., A. N. Ababneh, and Y. Xi (2016). "The effect of moisture transport on chloride penetration in concrete". In: *Construction and Building Materials* 125, pp. 1189–1195. ISSN: 0950-0618. DOI: 10.1016/j.conbuildmat.2016.08.124. URL: http://dx.doi.org/10.1016/j.conbuildmat.2016.08.124 (cit. on p. 4).

Johansson, H. (2011). *ConvergenceRate MATLAB function*. Göteborg, Sweden: Chalmers, Deptartment of Applied Mechanics (cit. on p. 17).

Lundgren, K. (2007). "Effect of corrosion on the bond between steel and concrete: an overview". In: *Magazine of Concrete Research* 59.6, pp. 447–461. ISSN: 0024-9831. DOI: 10.1680/macr.2007.59.6.447. URL: http://www.icevirtuallibrary.com/doi/10.1680/macr.2007.59.6.447 (cit. on p. 1).

MATLAB (2017). *Design of Experiments (DOE)*. URL: http://se.mathworks.com/help/stats/design-of-experiments-1.html?refresh=true (visited on 05/19/2017) (cit. on p. 18).

Montgomery, D. C. (2009). *Design and analysis of experiments*. 7th ed. Hoboken, New Jersey: John Wiley and sons, p. 656. ISBN: 978-0-470-39882-1 (cit. on p. 16).

Neville, A. M. and J. J. Brooks (2010). *Concrete Technology*. 2nd ed. Essex: Pearson Education, p. 442. ISBN: 978-0-273-73219-8 (cit. on p. 3).

Nilenius, F. (2014). "Moisture and Chloride Transport in Concrete: Mesoscale Modelling and Computational Homogenization." New Series No 3658, 29 pp. + papers. Doctoral dissertation. Chalmers University of Technology (cit. on pp. 1, 3, 4).

Nilenius, F., F. Larsson, K. Lundgren, and K. Runesson (2014a). "Computational homogenization of diffusion in three-phase mesoscale concrete". In: *Computational Mechanics* 54.2, pp. 461–472. ISSN: 0178-7675. DOI: 10.1007/s00466-014-0998-0. URL: http://link.springer.com/10.1007/s00466-014-0998-0 (cit. on pp. 1, 4).

Nilenius, F., F. Larsson, K. Lundgren, and K. Runesson (2014b). "Mesoscale modelling of crack-induced diffusivity in concrete". In: *Computational Mechanics* 55.2, pp. 359–370. ISSN: 01787675. DOI: 10.1007/s00466-014-1105-2 (cit. on p. 1).

Ottosen, N. S. and H. Petersson (1992). *Introduction to the finite element method*. Essex: Pearson Education, p. 410. ISBN: 978-0-13-473877-2 (cit. on pp. 9, 12).

ParaView (2017). *Parallel visualization application*. Version 5.2.0. Clifton Park, New York: Kitware Inc. URL: http://paraview.org (cit. on p. 4).

Parghi, A. and M. S. Alam (2016). "Seismic behavior of deficient reinforced concrete bridge piers confined with FRP – A fractional factorial analysis". In: *Engineering Structures* 126, pp. 531–546. ISSN: 01410296. DOI: 10.1016/j.engstruct.2016.08.011. URL: http://linkinghub.elsevier.com/retrieve/pii/S0141029616304126 (cit. on p. 16).

Petrie, C. S. and J. L. Williams (2005). "Comparative evaluation of implant designs: influence of diameter, length, and taper on strains in the alveolar crest". In: *Clinical Oral Implants Research* 16.4, pp. 486–494. ISSN: 09057161. DOI: 10.1111/j.1600-0501.2005.01132.x. URL: http://doi.wiley.com/10.1111/j.1600-0501.2005.01132.x (cit. on p. 16).

Saltelli, A., M. Ratto, T. Andres, F. Campolongo, J. Cariboni, D. Gatelli, M. Saisana, and S. Tarantola (2008). *Global Sensitivity Analysis: The Primer*. Chichester, UK: John Wiley & Sons, Ltd, p. 312. ISBN: 978-0-470-05997-5. DOI: 10.1002/9780470725184. URL: http://doi.wiley.com/10.1002/9780470725184.ch6%20http://doi.wiley.com/10.1002/9780470725184 (cit. on p. 16).

Tahershamsi, M., K. Zandi, K. Lundgren, and M. Plos (2014). "Anchorage of naturally corroded bars in reinforced concrete structures". In: *Magazine of Concrete Research* 66.14, pp. 729–744. ISSN: 0024-9831. DOI: 10.1680/macr.13.00276. URL: http://www.icevirtuallibrary.com/doi/10.1680/macr.13.00276 (cit. on p. 1).

A ConcreteCover function

```
classdef SVEclass < handle
  properties
        cover
        NodeCover
        a_cover
        row
        col
        Duration
        max_diff
        diff
    end

function ConcreteCover(obj,initialCondition,time)
            % Load the
            load([obj.path2Realization,'TopologyBundle_',num2str(obj.nx), ...
                '_',num2str(obj.realizationNumber),'.mat'],'NodeCoords')
            %Load a_store
            load([obj.path2Realization,obj.transientName,'.mat']);
            % needed for transparency for parfor since it is loaded
            NodeCoords = NodeCoords;
            obj.NodeCover = find(NodeCoords(:,4)≥ obj.cover & ...
                NodeCoords(:,4)< obj.cover+(obj.Lbox/obj.nx));
            obj.a_cover = a_store(obj.NodeCover(1):obj.NodeCover(end),1:end);
            [¬,n] = size(obj.a_cover);
            % Specify tolerance between a vector & initialCondition
            tol = 0.01;
            for i=2:n
                obj.diff(:,i-1) = obj.a_cover(:,i)-initialCondition;
                obj.max_diff(i-1,:) = max(obj.a_cover(:,i)-initialCondition);
            end

            [¬,j]=size(obj.diff);
            for i=1:j
                diff_sep = obj.diff(:,i);
                min_a = min(diff_sep(diff_sep>tol));
                if ¬isempty(min_a)
                   [obj.row,¬]=find(obj.diff==min_a);
                   obj.col=i;
                   break
                end
            end
            obj.Duration = obj.col*time.stepsize;
X = sprintf('The chloride exeeds by %d percent tolerance after %d years.', ...
    tol*100,obj.Duration);
            disp(X)
Y = sprintf( ...
'Node %d is the first node which exeeds in the cover plane with time step # ...
   %d' ...
```

```
,obj.row,obj.col);
            disp(Y)

                x = 1:n-1;
                actual_time = x*time.stepsize;
                % Just save the out put of the plot in a cell array
                %x-axis time
                Convergence_x=actual_time';
                %y-axis maxi diff between a and initial condition
                Convergence_y=obj.max_diff;
                savefile = [obj.path2Realization,'Converg_timestep_', ...
                  num2str(time.steps),'stepsize_',num2str(time.stepsize),'.mat'];
                save(savefile,'Convergence_x','Convergence_y','obj');
                plot(actual_time',obj.max_diff)
                xlabel('Time')
                ylabel('max(a-initialCondition)')
                title('timestep = 40, timestepsize=0.25')
                grid on
end
end
```